Entanglement revivals and scrambling for evaporating black holes

Levy B. N. Batista[1,*] Nicolò Bragagnolo[1,†] Rhys Holmes[2,‡] and S. Prem Kumar[1,§]

[1]*Centre for Quantum Fields and Gravity, Department of Physics, Swansea University, Singleton Park, Swansea, SA2 8PP, United Kingdom*

[2]*School of Physics and Astronomy, Cardiff University, 5 The Parade, Cardiff, CF24 3AA, United Kingdom*

(Received 18 May 2026; accepted 14 July 2026; published 6 August 2026)

We investigate the spreading of entanglement, and entanglement memory effects, in two-dimensional conformal field theory (CFT) propagating on evaporating black hole backgrounds. Memory effects leading to late-time spikes in mutual information for widely separated intervals are well known in CFTs admitting a quasiparticle description. In this work we examine the effect of black hole scrambling on late time mutual information spikes for disjoint intervals in free fermion CFT prepared in a thermofield double state. Late-time entanglement revival is driven by island-induced purification of modes in the union of the intervals. We show across two distinct 2D gravity models, Jackiw-Teitelboim (JT) gravity and the Russo-Susskind-Thorlacius (RST) model, that parametrically dialing up black hole scrambling time smooths out and suppresses entanglement spikes until they disappear at a critical scale, interpolating between free quasiparticle and maximal scrambling pictures. At the critical point, the interval lengths are exponential in black hole scrambling time. We further find a very closely related effect manifest as an entanglement dip for a single interval in a single-sided evaporating RST black hole.

DOI: 10.1103/z1j3-zq5g

I. INTRODUCTION

The scrambling of entanglement is a hallmark of quantum chaotic systems. First enunciated in the context of information loss and retrieval from black holes [1–3], how entanglement spreads and scrambles in quantum field theories (QFTs) is an interesting question in its own right. For QFTs in which excitations have a quasiparticle description, entanglement built into an atypical initial state for the quasiparticles can survive at relatively long separations and at late times [4]. A particularly useful and striking diagnostic test of this is provided by the time evolution of the mutual information between two well-separated finite intervals in $1+1$-dimensional conformal field theory (CFT) [4,5] which exhibits a late time spike. Such spikes are however absent in large-c holographic CFTs which are maximally scrambling [6,7].

Evaporating black holes bring a new element into the mix, as the black hole will additionally scramble the correlations built into the initial QFT matter state. Effective $1+1$-dimensional models such as Jackiw-Teitelboim (JT) gravity [8,9] coupled to a nongravitating CFT bath and the Russo-Susskind-Thorlacius (RST) model [10,11] provide a calculable framework to examine entanglement scrambling in general, by employing the generalized entropy and island formalism [12–15]. In this situation, there are potentially two timescales at play—the black hole scrambling time (at temperature β^{-1}),[1]

$$t_{\mathrm{scr}} = \frac{\beta}{2\pi}\log\frac{\Delta S_{\mathrm{BH}}}{c}, \tag{1.1}$$

where ΔS_{BH} is the entropy excess above the extremal value [16], and if the CFT is chaotic with a Lyapunov exponent λ_L then a CFT scrambling timescale $t_{\mathrm{CFT}} = \frac{1}{\lambda_L}\log c$. Free CFTs, and more generally CFTs with infinite higher spin conserved currents have vanishing Lyapunov exponents and correspondingly do not scramble ($t_{\mathrm{CFT}} \to \infty$) [17].

In this paper, we study free fermion CFT propagating in a $1+1$-dimensional black hole background. Our motivation stems from the scenario originally examined in [18] for the two-sided AdS_2 black hole in JT gravity coupled to Minkowski CFT baths in the thermofield double (TFD) state. In that work, the mutual information evolution of two

*Contact author: L.DNBatista@swansea.ac.uk
†Contact author: nicolo.bragagnolo@swansea.ac.uk
‡Contact author: HolmesRA1@cardiff.ac.uk
§Contact author: s.p.kumar@swansea.ac.uk

[1]The extra factor of c in the argument of the log arises from the fact that there are c CFT degrees of freedom and therefore t_{scr} is correspondingly shorter [12].

disjoint finite intervals A_L and A_R, placed in the left and right copies of the CFT baths showed a peak for well separated intervals at late times.[2] In particular, at high enough temperatures and for large enough intervals, so $t_{\rm scr}$ is negligible in the limit, the entanglement entropy $S(A_L \cup A_R)$ behaves identically to that of free fermion CFTs on the half-line, BCFT_L and BCFT_R, prepared in a TFD state with the boundaries acting as reflecting mirrors for the quasiparticles. $S(A_L \cup A_R)$ initially grows until it saturates at the corresponding thermal result. The inclusion of an island accounts for an entropy dip (equivalently, a spike in the mutual information $I(A_L, A_R)$) *well after* entanglement equilibrium has been reached. This purification can be quantitatively captured via a geometric or ray optics description of Hawking modes entering the region $A_L \cup A_R$ at the same time as their maximally entangled partner modes enter the island, or equivalently in the BCFT picture, when the partner modes enter $A_L \cup A_R$ after reflection from the boundary mirror.

We will examine below how the picture above is affected by the finite scrambling time of the black hole. Across the two setups—the AdS_2 black hole within JT gravity, and the asymptotically flat black hole in the RST model—we find that the mutual information spike is smoothed out and reduced by the black hole scrambling effect, disappearing entirely below a critical value of the interval size,

$$\boxed{L_{\rm crit} = c_1 \frac{\beta}{2\pi} e^{\frac{2\pi}{\beta} t_{\rm scr}} + c_2 t_{\rm scr} + \mathcal{O}(\beta),} \tag{1.2}$$

where $c_{1,2}$ are $\mathcal{O}(1)$ dimensionless theory- and state-dependent coefficients, and we work to leading order in a high temperature expansion $\beta \ll t_{\rm scr}, L$ where L is the interval size. As a bonus we find an additional critical scale for large intervals wherein a transient period prior to the entanglement the entropy dip (dubbed regime (II) in [18]) disappears as the scrambling time is dialled up.

We further find a closely related phenomenon—an entanglement entropy dip in a single, finite interval of radiation in the single-sided evaporating black hole in the RST model. We find that the dip in this case is also smoothed out and disappears below a critical interval length given by (1.2).

Our paper is organized as follows: In Sec. II we review the well studied setup of JT gravity coupled to non-gravitating CFT baths, and proceed to the analytical evaluation of the mutual information of two intervals in the TFD state and plotting the results for different numerical values of β, scrambling time, and interval length. Section III deals with the RST model in entirety. We first review general aspects of the RST model, and discuss the phenomenon of entanglement dips in the single-sided evaporating background, moving on finally to the eternal black hole solution to study entanglement revivals in the TFD state. We conclude with a summary and directions for future work in Sec. IV.

[2]For simplicity, we consider only the symmetric case, i.e., when the intervals A_L and A_R are identical.

II. JT BLACK HOLE COUPLED TO MINKOWSKI RADIATION BATHS

We first examine the eternal black hole in AdS_2 within JT gravity [8,9], coupled to two non-gravitating Minkowski reservoirs. A 2D dilaton gravity model, JT gravity describes the low-energy dynamics near the horizon of near-extremal black holes in four dimensions. The 2D dilaton is proportional to the area of the two-sphere in the higher dimensional setting [19], and its value at the horizon determines the Bekenstein-Hawking (BH) entropy of the black hole.

In this setup, the black hole is in thermal equilibrium with the radiation bath whose degrees of freedom are described by a CFT, which we take to be the free fermion theory for definiteness. These massless fields propagate across the AdS and Minkowski regions with transparent boundary conditions on the regularized AdS boundary that is glued onto the non-gravitating region.

A. Setup and notation

Let us now set the notation for the rest of this section. As shown in Fig. 1 above we consider two intervals, A_L with end points 2_L and 1_L, and A_R whose end points are 1_R and 2_R, defined on the same Cauchy slice. We take Minkowski bath coordinates (t, x) with spatial coordinate $x \geq 0$ and t, the bath time. They can be extended to the AdS region outside the black hole by taking $x \in \mathbb{R}$, and identifying t with Schwarzschild time. We then define appropriate null coordinates,

$$x_R^\pm = t \pm x, \qquad x_L^\pm = -t \pm x + \frac{i\beta}{2}, \tag{2.1}$$

on the right (R) and left (L) regions respectively. As required for the Hartle-Hawking initial state, we have taken $t_L = -t_R + i\beta/2$. These lead to Kruskal-Szekeres (KS) coordinates that cover the whole spacetime,

$$w^\pm = \pm e^{\pm 2\pi x^\pm/\beta}. \tag{2.2}$$

The left and right (future) horizons are at $w^+ = 0$ and $w^- = 0$, respectively, and the AdS_2 metric in these coordinates is

$$ds^2 = -\frac{4dw^+ dw^-}{(1 + w^+ w^-)^2}. \tag{2.3}$$

The AdS_2 conformal boundaries are at $w^+ w^- = -1$, and the dilaton profile is given by

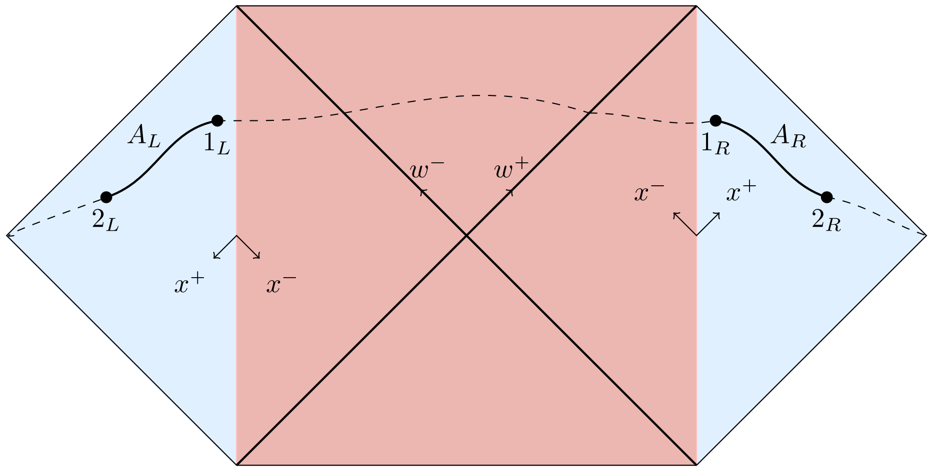

FIG. 1. The Penrose diagram describing an eternal black hole in AdS_2 glued onto two half Minkowski baths. The intervals A_L and A_R are contained in the nongravitating regions and are part of the same Cauchy slice (dashed) in the resulting spacetime.

$$\phi = \phi_0 + \frac{2\pi\phi_r}{\beta}\frac{1-w^+w^-}{1+w^+w^-}. \tag{2.4}$$

In JT gravity, the BH entropy of the black hole is given by the value of the dilaton at the horizon,

$$S_{\rm BH} = \frac{\phi}{4G_N}\bigg|_{w^-=0} = S_0 + \frac{\pi c}{6\beta k}, \tag{2.5}$$

where $k \equiv G_N c/3\phi_r$ is the JT parameter, and $S_0 = \frac{\phi_0}{4G_N}$ is the extremal value of the entropy. The parameter k has dimensions of inverse length and in units where the AdS radius is set to one, $k \ll 1$ to ensure the validity of the semiclassical approximation.

B. Entanglement revivals and critical disappearance

To understand how the information spreads across spacetime, we consider the mutual information between the intervals A_L and A_R,

$$I(A_L, A_R) = S(A_L) + S(A_R) - S(A_L \cup A_R), \tag{2.6}$$

where $S(A)$ is the entanglement entropy associated to an interval A. The mutual information provides a measure of how correlated A_L and A_R are. Furthermore, unlike entanglement entropy it is free of UV divergences.

To compute this mutual information in the system coupled to dynamical gravity we need the individual fine-grained or generalized entropies for $A_{L,R}$ and $A_L \cup A_R$. For any interval A, this is given by the island formula,

$$S(A) = \min \mathrm{ext}_{\partial I}\left[\sum_{\partial I}\frac{\mathrm{Area}(\partial I)}{4G_N} + S_{\rm CFT}(I \cup A)\right], \tag{2.7}$$

where we admit the inclusion of additional intervals I, the islands, with boundaries ∂I, so-called quantum extremal surfaces (QES) corresponding to points in the 2D effective gravity models. $S_{\rm CFT}(I \cup A)$ accounts for the semiclassical von Neumann entropy of the quantum fields on the region $I \cup A$.[3] The CFT computation of this is standard, and for free fermions the exact result for arbitrary choices of intervals is known (see [20] for a review).

1. No-island saddle and late times

Given the symmetric choice of the intervals $A_{L,R}$, the KS coordinates of their end points 2_L, 1_L, 1_R, and 2_R are

$$\begin{cases} w^{\pm}_{1R} = w^{\mp}_{1L} = \pm e^{2\pi(\pm t + a)/\beta}, \\ w^{\pm}_{2R} = w^{\mp}_{2L} = \pm e^{2\pi(\pm t + b)/\beta}. \end{cases} \tag{2.8}$$

By construction, we have that $S(A_L) = S(A_R)$. In the TFD state all single-sided correlators are given by their thermal equilibrium values. Entanglement and its growth only manifests in two-sided observables and correlation functions. Further, inclusion of a potential island contribution only increases the fine-grained entropy, as the area term represents a large contribution. Therefore,

$$S(A_R) = S(A_L) = \frac{c}{3}\log\sinh\frac{\pi}{\beta}L, \qquad L \equiv b - a. \tag{2.9}$$

For $S(A_L \cup A_R)$ on the other hand, we must consider the competition between the island and no-island (Hawking)

[3] In principle, nothing prevents the extremization in Eq. (2.7) from resulting in multiple island saddles. Thus, we complete the prescription by picking the one that minimizes the generalized entropy.

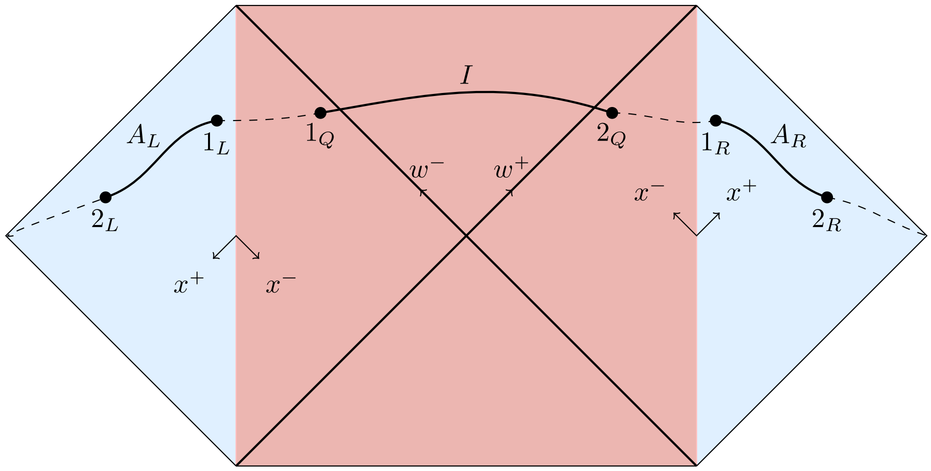

FIG. 2. In the generalized entropy proposal, one of the possible saddles contains an island I, which will "perturb" the entanglement equilibrium of region $A_L \cup A_R$ at late times, exhibiting a memory effect when the black hole scrambling is subdominant.

saddles. In the Hawking or no-island saddle for late times after a short period of linear growth $S_\varnothing(A_L \cup A_R)$ approaches the equilibrium value[4] determined by Eq. (2.9) (see [18] for exact expressions),

$$S_\varnothing(A_L \cup A_R) \to 2S(A_{L,R}). \tag{2.10}$$

Therefore the mutual information vanishes at late times in the no-island saddle. On the other hand the island contribution to $S(A_L \cup A_R)$ results in a late-time dip in the entropy and spike in the mutual information for times $a < t < b$ as demonstrated in [18] in the high temperature limit $L/\beta \gg 1$, and when the scrambling time is also negligible $a, b, L \gg t_{\rm scr}$.

2. Black hole scrambling time

In the present analysis our goal is to understand the effect of finite scrambling time on the entanglement dip or mutual information spike. To this end, it will be useful and natural to define the small dimensionless parameter s,

$$s \equiv \frac{\beta k}{2\pi} \ll 1, \tag{2.11}$$

in terms of which the black hole scrambling time can be expressed as

$$t_{\rm scr} = \frac{\beta}{2\pi} \log \frac{\Delta S_{\rm BH}}{c} = \frac{\beta}{2\pi}\left[\log \frac{1}{s} + \mathcal{O}(1)\right]. \tag{2.12}$$

[4]This is valid for small intervals with $b < 3a$, while for $b > 3a$ the island saddle will possibly affect also the early growth regime. This will be discussed in detail in Sec. II C 1.

A quick route to this result for the scrambling time is by calculating how much boundary time has elapsed before a null diary sent in from the AdS_2 boundary reaches the QES and becomes recoverable in the radiation.

We now want to work in a regime where scrambling time is non-negligible compared to other length and timescales L, a, b, t, and is parametrically larger than the thermal time

$$t_{\rm scr} \gg \frac{\beta}{2\pi}, \tag{2.13}$$

Note that small s automatically implies that scrambling time is much bigger than the thermal timescale. Below, we explain what happens to the mutual information $I(A_L, A_R)$ as we vary s, L, and β.

3. The critical length

First we will show that there is a critical size for the length of the intervals $A_{L,R}$ below which the dip in the entanglement entropy of $A_L \cup A_R$ will disappear. The idea is to find the minimum entropy as described by the island saddle and see under which conditions this is larger than the thermal entropy of both intervals. The minimal island saddle has two QESs, which we denote by 1_Q on the left side, and 2_Q on the right, as depicted in Fig. 2. By symmetry, we have the relation

$$w^{\pm}_{1_Q} = w^{\mp}_{2_Q}. \tag{2.14}$$

The exact expression for the generalized entropy as a function of the QES locations can be written using the exact formulae for CFT entanglement entropy for free fermions [18,20] by labeling the six points $\{2_L, 1_L, 1_Q, 2_Q, 1_R, 2_R\}$ along the Cauchy slice as $\mu = 1, 2, \ldots 6$ from left to right,

$$S_I(A_L \cup A_R) = 2S_0 + \frac{\pi c}{6\beta k}\sum_{\mu=3,4}\frac{1-w_\mu^+ w_\mu^-}{1+w_\mu^+ w_\mu^-} - \frac{c}{12}\sum_{\mu\neq 3,4}\log w_\mu^+ w_\mu^- \\ - \frac{c}{6}\sum_{\mu<\nu}(-1)^{\mu-\nu}\log\left[-(w_\mu^+ - w_\nu^+)(w_\mu^- - w_\nu^-)\right] - \frac{c}{6}\sum_{\mu=3,4}\log(1+w_\mu^+ w_\mu^-). \tag{2.15}$$

The first two terms on the right-hand side arise from the dilaton evaluated at the QESs, the third and final terms originate from conformal factor contributions at end points in the bath and the QESs in the gravitating region. In what follows, we will work in the high temperature limit so that the extremal entropy S_0 is negligible in comparison to the thermal entropy of the black hole. In general this is quite a complicated expression to extremise with respect to the QES locations $w^\pm_{1_Q}$ or $w^\pm_{2_Q}$. However, in the high temperature limit (2.13), and with $a < t < b$, the coordinates satisfy,

$$|w^\pm_{2_R}|, |w^+_{1_R}| \gg 1. \tag{2.16}$$

In addition, the QES is always expected to be close to the horizon in the semiclassical limit, and so we may reliably assume, say, for the right QES location,

$$|w^-_{2_Q}| \ll |w^+_{2_Q}|, \qquad |w^+_{2_Q} w^-_{2_Q}| \ll 1, \tag{2.17}$$

which we can verify *a posteriori*. Finally, the ordering of points along the Cauchy slice in the high temperature limit implies

$$w^+_{2_R} \gg w^+_{1_R} \gg w^+_{2Q}. \tag{2.18}$$

With these assumptions (consistent with the semiclassical limit) in place, extremizing the generalized entropy with respect to the QES positions leads to the following equations:

$$\frac{s+1}{s}w^+_{2_Q} = \frac{1}{w^-_{2_Q} - w^-_{1_R}},$$
$$\frac{s+1}{s}w^-_{2_Q} = \frac{1}{w^+_{2_Q}} - \frac{1}{w^+_{2_Q} - w^+_{1_L}} + \frac{1}{w^+_{2_Q} - w^+_{2_L}} - \frac{1}{w^+_{1_R}}. \tag{2.19}$$

For the moment we retain s in the numerator of the left-hand side, but eventually we want to consider $s \ll 1$. The equations for the QES (2.19) can be solved readily, and yield two sets of roots, one of which is physically relevant[5] and takes on a compact form [after using the condition $e^{4\pi a/\beta} \gg s/(s+1)$],

$$w^+_{2_Q} = \sqrt{e^{2\pi(b+a-2t)/\beta}\sinh^2\frac{\pi}{\beta}(b-a) + \frac{2s}{s+1}e^{\pi(b-a)/\beta}\sinh\frac{\pi}{\beta}(b-a)} - e^{\pi(b+a-2t)/\beta}\cosh\frac{\pi}{\beta}(b-a). \tag{2.20}$$

This expression interpolates between early and late times within the time interval $a < t < b$ during which the entanglement dip is expected to occur,

$$w^+_{2_Q} \approx \begin{cases} \frac{s}{s+1}e^{2\pi(t-a)/\beta} & a < t \lesssim \frac{a+b}{2} + \frac{1}{2}t_{\rm scr}, \\ \sqrt{\frac{s}{s+1}}e^{\pi(b-a)/\beta} & \frac{a+b}{2} + \frac{1}{2}t_{\rm scr} \lesssim t < b. \end{cases} \tag{2.21}$$

At this point, it is useful to make contact with the nomenclature introduced in [18] where, ignoring $t_{\rm scr}$ for the moment, the following relevant temporal regimes were identified for the separate cases $b > 3a$

$$({\rm II}) = \left\{a < t < \frac{1}{2}(b-a)\right\}$$
$$({\rm III}) = \left\{\frac{1}{2}(b-a) < t < \frac{1}{2}(a+b)\right\}$$
$$({\rm IV}) = \left\{\frac{1}{2}(b+a) < t < b\right\}, \tag{2.22}$$

and $b < 3a$

$$({\rm III}) = \left\{a < t < \frac{1}{2}(a+b)\right\}$$
$$({\rm IV}) = \left\{\frac{1}{2}(b+a) < t < b\right\}. \tag{2.23}$$

For small s, ignoring s in the denominator, the first line of (2.21) precisely matches the QES location in [18] that covers the regimes (II) and (III) (across both cases above), while the second line matches the solution in regime (IV).[6]

[5] The other root is negative and must be discarded.

[6] Furthermore, in the IR limit, the eternal AdS_2 black hole coupled to Minkowski baths can be argued to be dual to two copies of (free) CFT with boundary (BCFT) prepared in the thermofield double state. The entanglement entropy of two intervals in the BCFT system follows from a four-point correlator of twist fields. The different temporal regimes identified are controlled by different channels dominating the 4-point function. In the language of [18] the QES solutions capture the entanglement evolution governed by the BCFT channels (3) and (4) which yield light cone singularities in free CFTs.

It is easy to check that the condition $|w^-_{2_Q}| \ll |w^+_{2_Q}|$ is automatically satisfied in these regimes, while the requirement that $|w^+_{2_Q} w^-_{2_Q}| \ll 1$ needs $s \ll 1$.

Since the late time entropy in the no-island saddle is constant and equal to the thermal entropy, it is natural to consider the difference,

$$\Delta S \equiv S_I(A_L \cup A_R) - S_\varnothing(A_L \cup A_R). \tag{2.24}$$

For late times this is essentially minus the mutual information. The exact expression for the no-island value of the entropy is

$$S_\varnothing(A_L \cup A_R) = -\frac{c}{12}\sum_\mu \log w^+_\mu w^-_\mu - \frac{c}{6}\sum_{\mu<\nu}(-1)^{\mu-\nu}\log[-(w^+_\mu - w^+_\nu)(w^-_\mu - w^-_\nu)], \tag{2.25}$$

where the sums run only over the 4 end points in the bath $\{2_L, 1_L, 1_R, 2_R\}$ labeled by μ, $\nu = 1, 2, 5, 6$. Then, the non-negligible contributions to ΔS can be compactly identified as[7]

$$\Delta S = \frac{c}{6}\left[\frac{1}{s}(1 - 2w^+_{2_Q} w^-_{2_Q}) + 2\log\frac{w^+_{2_Q} - w^-_{2_R}}{w^+_{2_Q} - w^-_{1_R}} + 2\log\frac{w^+_{2_Q}}{1 + w^+_{2_Q}(1 + 1/s)(w^-_{1_R} - w^-_{2_R})}\right]. \tag{2.26}$$

In the high temperature limit and deep within the interval $a < t < b$, we can use $|w^+_{2_Q}| \gg |w^-_{1_R}|$ and $|w^-_{2_R}| \gg 1$ to write

$$\Delta S \approx \frac{c}{6}\left[\frac{1}{s}\left(\frac{1-s}{1+s} + 2w^+_{2_Q} e^{2\pi(a-t)/\beta}\right) - 2\log(1 + 1/s) + 2\log\left(e^{2\pi(t-b)/\beta} + \frac{1}{w^+_{2_Q}}\right)\right]. \tag{2.27}$$

To determine the critical size of the interval below which the entanglement dip disappears, we must find the minimum value of ΔS as a function of time and require that $\Delta S_{\min} \geq 0$. Expecting a minimum near the midpoint of the interval $t = (a + b)/2$ we find that using *either* the early *or* the late time approximations for $w^+_{2_Q}$ in, in the small s limit, yields the same location for the minimum of Eq. (2.27),

$$t_{\min} \approx \frac{a+b}{2} + \frac{\beta}{4\pi}\log\frac{1}{s}. \tag{2.28}$$

Although this result is at the edge of the validity of either the early or late time approximation for w^+_{2Q}, we find that it closely matches the results from the complete expressions (2.15), (2.20), and (2.25). We see above that the dip time is shifted from the midpoint of the interval by an amount fixed by the scrambling time of the black hole. Substituting t in Eq. (2.27), we obtain the value of $\Delta S_{\min}$,

$$\Delta S_{\min} = \frac{c}{6}\left(-\frac{2\pi}{\beta}L + \frac{1}{s} - \log\frac{1}{s} + \mathcal{O}(s^0)\right), \tag{2.29}$$

where $L = b - a$. Therefore the entanglement dip will vanish when $\Delta S_{\min} \geq 0$ which in turn implies

$$L \leq L_{\text{crit}} = \frac{\beta}{2\pi}\left(\frac{1}{s} - \log\frac{1}{s} + \mathcal{O}(s^0)\right). \tag{2.30}$$

[7]As indicated previously, for simplicity we ignore the extremal entropy S_0 in the high temperature limit.

The critical length can also be reexpressed in terms of the scrambling time,

$$L_{\text{crit}} \approx \frac{\beta}{2\pi}\exp\left(\frac{2\pi}{\beta}t_{\text{scr}}\right) - t_{\text{scr}}. \tag{2.31}$$

This illustrates that in order to see long-distance correlations in the Hawking radiation, we must consider length/timescales that are at least exponential in scrambling time.

C. Mutual information

A dip in entanglement entropy corresponds to a spike in the mutual information $I(A_L, A_R)$, indicating that the correlations spread across spacetime as if they are being carried away by free quasiparticles [4]. We now evaluate $I(A_L, A_R)$ using the exact expressions (2.9) together with (2.25) and (2.15) for the no-island and island entropies, i.e. $S_\varnothing(A_L \cup A_R)$ and $S_I(A_L \cup A_R)$, respectively.

In the following, we will first focus on the "small interval" scenario in which the interval length is smaller than the distance of the midpoint of the interval from the boundary

$$R_c \equiv \frac{b+a}{2}, \qquad L < R_c \Rightarrow b < 3a. \tag{2.32}$$

This regime, as noted in [18], is when the dip appears in isolation, well after the entropy of entanglement has plateaued. It is the only effect of the island saddle which results in a spike or blip in the mutual information. We will

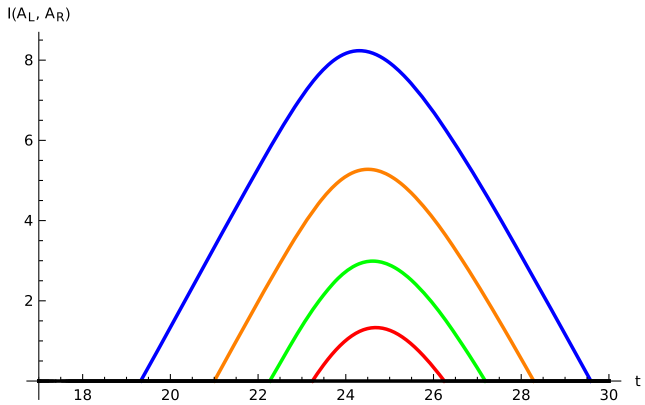

FIG. 3. Mutual information $I(A_L, A_R)$ as a function of time t for $a = 16$, $b = 30$, and $\beta = 2\pi$. The late-time spike is displayed for $s = 0.15$ (blue), $s = 0.1$ (orange), $s = 0.08$ (green), and $s = 0.07$ (red). For $s = 0.06$, scrambling effects completely dominate the correlation spreading process, and there is no spike. The black line corresponds to vanishing mutual information for values of $s \leq s_{\mathrm{crit}} \approx 0.06$, where the Hawking or no-island saddle dominates at all times.

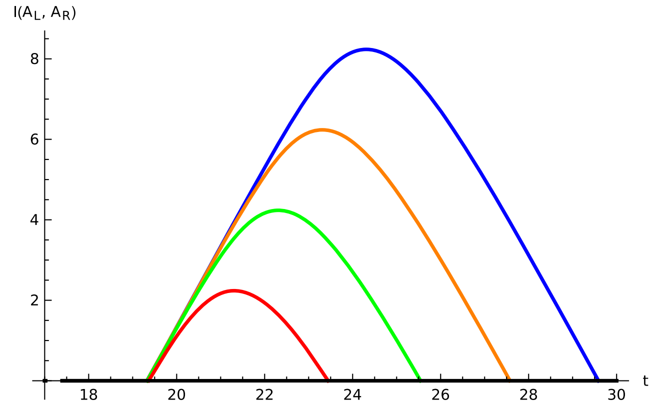

FIG. 4. Mutual information $I(A_L, A_R)$ as a function of time t for $s = 0.15$, $a = 16$, and $\beta = 2\pi$. We show the late-time spike for $b = 30$ (blue), $b = 28$ (orange), $b = 26$ (green), and $b = 24$ (red). The spike disappears when we set $b = 22$, and we note that $L_{\mathrm{crit}} \approx 6$ as dictated by Eq. (2.30). The black line corresponds to the mutual information for values of $L \leq L_{\mathrm{crit}}$, where the island saddle is subdominant at all times.

treat separately the case $L > R_c$ or $b > 3a$ in the next subsection, since it reveals a second critical regime for scrambling.

Our results show that entanglement memory is progressively lost as we decrease the parameter s, i.e., with increasing scrambling time. Figure 3 shows that the spike in the mutual information, originating from the island contribution, is lower and narrower as s is decreased for a fixed value of the interval length $L = 14$ and $\beta = 2\pi$.[8] Interestingly, if we solve Eq. (2.30) for s, with $L = 14$ and $\beta = 2\pi$, we find $s = 0.059$ for the critical value of s at which correlations should vanish, agreeing with the behavior of the mutual information observed in Fig. 3. For any s smaller $s \lesssim 0.06$, the correlations are completely scrambled.

Additionally, we can find when the entanglement revivals start and end, considering corrections due to scrambling. Explicitly, the end points of the spike turn out to be

$$t_{\mathrm{in}} = a + \frac{1}{2k} + \mathcal{O}(\beta),$$
$$t_{\mathrm{fin}} = b - \frac{1}{2k} + \frac{\beta}{2\pi}\left(\log\frac{1}{s} + \mathcal{O}(s^0)\right). \qquad (2.33)$$

Therefore, although the peak time deviates from $t = (a + b)/2$ as we vary s, Eq. (2.28) shows that the spike remains symmetric up to high-temperature corrections about its peak at $t_{\mathrm{min}} = (t_{\mathrm{in}} + t_{\mathrm{fin}})/2$. Note that, in this regime, t_{in} only depends on a while t_{fin} only depends on b. Thus, for instance, varying b has no effect on t_{in}, as evident from the curves in Fig. 4.

Next, fixing s and β, we investigate how mutual information responds to variations of L. We do this by fixing the end point a and decreasing b. In Fig. 4, we plot $I(A_L, A_R)$ after the initial correlations between the intervals are lost, focusing only on the entanglement revivals. For L greater than the critical value L_{crit} determined by Eq. (2.30), the spikes start at the same time determined by the location of end point a, although their maximum point is shifted to the left as b decreases. The spikes preserve their shape when s and L are varied, but this is not the case when we vary β for fixed s and L as shown in Fig. 5. Decreasing β,

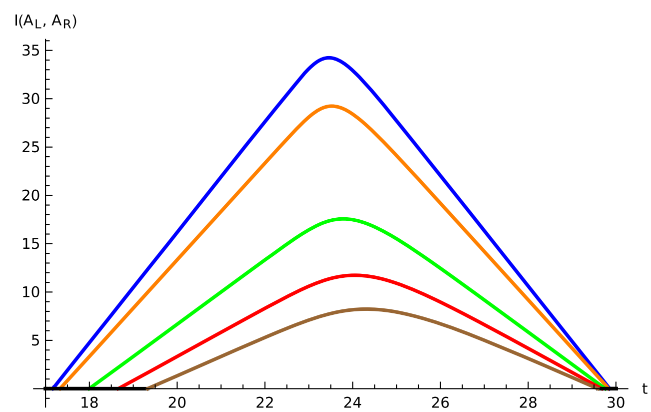

FIG. 5. Mutual information $I(A_L, A_R)$ as a function of time for $s = 0.15$, $a = 16$, and $b = 30$ for different temperatures, $\beta/2\pi = 0.35$ (blue), $\beta/2\pi = 0.4$ (orange), $\beta/2\pi = 0.6$ (green), $\beta/2\pi = 0.8$ (red), and $\beta/2\pi = 1$ (brown). We only display the region where entanglement revivals occur. The black line represents the portion of time where the mutual information is dominated by the Hawking saddle.

[8]Numerically small values of β are problematic as they lead to very large exponents in our expressions, so we do not go deep into the high temperature limit.

while keeping other parameters fixed, we recover the sharp symmetric profile observed in [18] in the high temperature, large interval limit.

Note that the parameter s depends on both β and k, so we can keep it constant by scaling β and the JT parameter k while keeping their product fixed, and ensuring that $k \ll 1$ (recalling that we have set the AdS radius to unity) [13]. For fixed L and s, Eq. (2.30) shows that the late-time spikes can be flattened by decreasing the temperature. This can be understood as progressively reducing the correlations shared by the intervals in the TFD state, making it easier for the black hole to scramble them.

1. Additional critical scrambling for $b > 3a$ case

In [18] it was shown that for symmetric intervals satisfying $b > 3a$, or $L > R_c$, there is an additional regime (II), in which the island saddle starts dominating over the Hawking saddle *before* the entanglement plateau is reached, and whose effect is to slow down the early-time entanglement entropy growth. This regime was considered in [18] in the limit $L \gg t_{\mathrm{scr}}$, and extends for $a < t < \frac{b-a}{2}$, following which, for $\frac{b-a}{2} < t < b$ [regime (III)] the island saddle produces an entanglement dip exactly as in the case $b < 3a$ analysed previously, with minimum at $t = \frac{a+b}{2}$.[9]

The analytic results for the QES in Sec. II B 3 are valid for $a < t < b$ and for both the cases $b > 3a$ and $b < 3a$. In the large interval situation with $b > 3a$, the time $t_{\mathrm{in}} \simeq a + \frac{1}{2k}$ becomes the time at which the island saddle starts dominating over the Hawking one in the regime (II) so the mutual information starts falling a bit slower than in the no-island saddle. A striking result is that, taking into account scrambling effects, the regime (II) starts later with respect to the BCFT prediction, and this regime itself shrinks as scrambling time increases. In particular, there is a critical parameter $s_{\mathrm{crit}}^{(\mathrm{II})}$ below which the regime (II) disappears entirely in favor of the early-time entropy growth regime (I), and this critical point can be found by equating t_{in} with the starting point of regime (III), i.e.

$$a + \frac{1}{2k} = \frac{b-a}{2} \Rightarrow s_{\mathrm{crit}}^{(\mathrm{II})} = \frac{\beta}{2\pi} \frac{1}{b-3a}. \qquad (2.34)$$

In terms of the interval length L and the distance of the interval midpoint from the boundary R_c, this condition can be reexpressed as

$$s_{\mathrm{crit}}^{(\mathrm{II})} = \frac{\beta}{4\pi} \frac{1}{L - R_c}, \qquad (2.35)$$

[9] For context, the beginning of the entanglement dip falls in regime (III) and its subsequent rise after the minimum at $t_{\mathrm{min}} = \frac{a+b}{2}$ in regime (IV) [18].

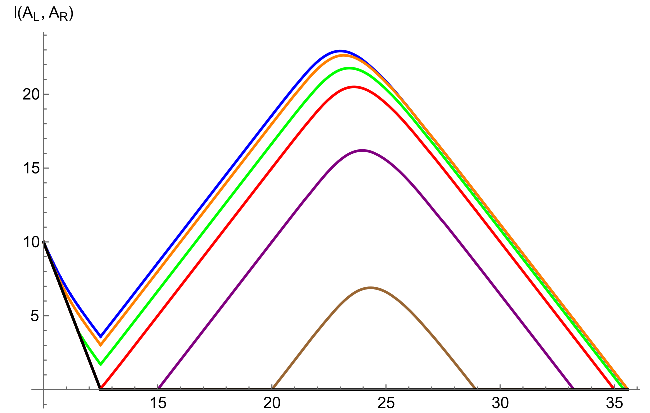

FIG. 6. Mutual information $I(A_L, A_R)$ as a function of time t for $a = 10$, $b = 35$, and $\beta = 2\pi$. The evaluation of $I(A_L, A_R)$ is displayed for $s = 0.7$ (blue), $s = 0.5$ (orange), $s = 0.3$ (green), $s = 0.2$ (red), $s = 0.1$ (purple), $s = 0.05$ (brown), and $s = 0.035$ (black). The red curve corresponds to $s_{\mathrm{crit}}^{(\mathrm{II})} = 0.2$ and the black line corresponds to the mutual information entirely determined by the Hawking/no-island saddle.

where L is necessarily larger than R_c. In Fig. 6, we plot the mutual information $I(A_L, A_R)$ for a fixed choice of interval satisfying $b > 3a$ and for several values of the scrambling parameter s: as expected, for $s < s_{\mathrm{crit}}^{(\mathrm{II})}$, the early linear decrease of mutual information is entirely due to the Hawking saddle.

III. ENTANGLEMENT REVIVALS IN THE RST MODEL

We now turn to a discussion of finite interval effects in the RST model. The RST model is a soluble 2D dilaton gravity model coupled to a large-N number of free fields and is a variant of the Callan-Giddings-Harvey-Strominger (CGHS) model [21]. It is an interesting toy model for studying Hawking evaporation in asymptotically flat spacetime. The generalized entropy formalism and the island paradigm, accompanied by a Page curve can be shown to arise from replica wormhole computations of the fine-grained entropy of entanglement of Hawking modes [15] in this background. One of the features of this model is that the geometry has a boundary, much like the origin of space in radial coordinates, where one imposes reflecting boundary conditions for matter fields propagating on the background [11]. The calculation of the von Neumann entropy of massless fields on such a background proceeds similarly to BCFT in two dimensions. Below we review some basic features of the RST model, before moving to an analysis of the finite interval problem for the single-sided evaporating black hole and the two-sided eternal black hole, both of which will exhibit entanglement dips for distinct reasons.

A. Brief review of RST model

The classical action of the RST model [10,11] is given by

$$S_{\mathrm{cl}} = \frac{1}{2\pi}\int d^2w\sqrt{-g}\left[e^{-2\phi}(R + 4(\nabla\phi)^2 + 4\lambda^2) - \frac{N}{24}\phi R - \sum_{k=1}^{N} i\bar{\psi}_k \nabla\!\!\!/ \psi_k\right], \tag{3.1}$$

where ϕ is the dilaton field and $\{\psi_k\}$ are N matter fields which we take to be massless Dirac fermions. The matter fields, in principle, can be replaced by any CFT with central charge N. The action (3.1) without the linear ϕR term yields the CGHS model [21]—two-dimensional dilaton gravity theory describing the low-energy physics governing the radial modes of a near extremal four-dimensional magnetically charged black hole. The length scale λ^{-1} accounts for the magnetic charge of the four-dimensional black hole, and from now on we will set $\lambda = 1$. A consistent semiclassical approximation can be implemented by taking the large-N limit, specifically $N \to +\infty$ with $Ne^{2\phi}$ fixed. At leading order in $1/N$, it turns out that the quantum fluctuations of the dilaton and the metric are negligible, and we need only to include the effect of the conformal anomaly due to matter fields i.e.

$$S_{\mathrm{anom}} = -\frac{N}{96\pi}\int d^2w\sqrt{-g}R\square^{-1}R. \tag{3.2}$$

The linear ϕR counterterm, distinguishing the RST from the CGHS action, has been added to make the model analytically tractable in the large-N limit, and it has been seen numerically [22,23] that this fine-tuned counterterm does not change the physics of the model qualitatively.

Going to the conformal gauge $ds^2 = -e^{2\rho}dw^+dw^-$, with $w^\pm = w^0 \pm w^1$ and $R_{+-} = -2\partial_+\partial_-\rho$, the large-$N$ effective action becomes

$$S_{\mathrm{eff}} = \frac{1}{2\pi}\int d^2w\left[e^{-2\phi}(4\partial_+\rho\partial_-\rho - 8\partial_+\phi\partial_-\phi + 2e^{2\rho}) + \frac{N}{6}(\rho-\phi)\partial_+\partial_-\rho + \sum_{k=1}^{N} i(\psi_{k+}\partial_-\psi_{k+} + \psi_{k-}\partial_+\psi_{k-})\right], \tag{3.3}$$

where $\psi_{k\pm}$ are left- and right-moving fermions. At this point, it is convenient to perform the following field redefinitions,

$$\Omega = \frac{12}{N}e^{-2\phi} + \frac{\phi}{2} - \frac{1}{4}\log\frac{48}{N},$$
$$\chi = \frac{12}{N}e^{-2\phi} + \rho - \frac{\phi}{2} + \frac{1}{4}\log\frac{3}{N}, \tag{3.4}$$

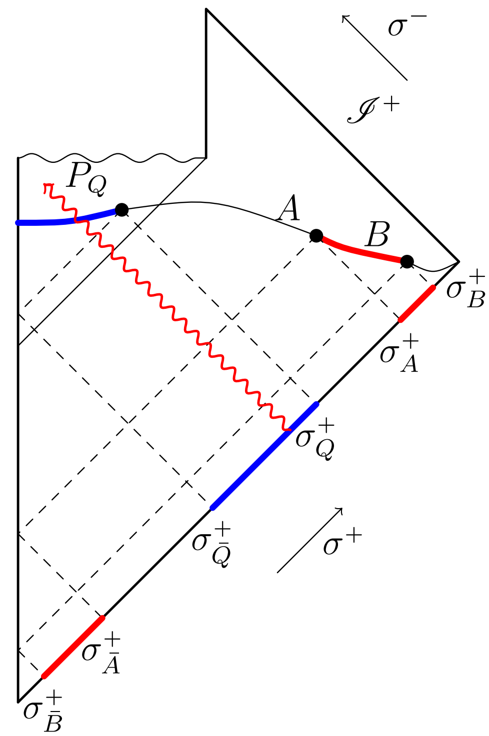

FIG. 7. The Penrose diagram depicting an evaporating black hole, produced by a shockwave (red wavy line) insertion at $\sigma^+ = 0$, as described by the solution (3.13) of the RST model. The region R and its projections onto $\mathscr{I}^-$ are shown in red, whereas the island and its corresponding null projection are shown in blue.

where the field Ω plays the role of the area of the two-sphere of the four-dimensional black hole, therefore it is the RST gravity counterpart of the JT gravity dilaton.

In terms of these fields the action takes the form,

$$S_{\mathrm{eff}} = \frac{N}{12\pi}\int d^2w\left(\partial_+\Omega\partial_-\Omega - \partial_+\chi\partial_-\chi + e^{2\chi-2\Omega} + \frac{6}{N}\sum_{k=1}^{N} i(\psi_{k+}\partial_-\psi_{k+} + \psi_{k-}\partial_+\psi_{k-})\right), \tag{3.5}$$

which scales with an overall factor of N in the large-N limit, with Ω and χ held fixed.

The field Ω has a minimum as a function of ϕ, where $\Omega_{\mathrm{min}} = 1/4$. A smaller value of Ω would require a complex dilaton, which would be problematic,[10] implying the well-known condition

$$\Omega \geq \frac{1}{4}. \tag{3.6}$$

[10] A complex dilaton would give a negative coefficient of the Einstein-Hilbert term, thus a violation of unitarity in the semi-classical description.

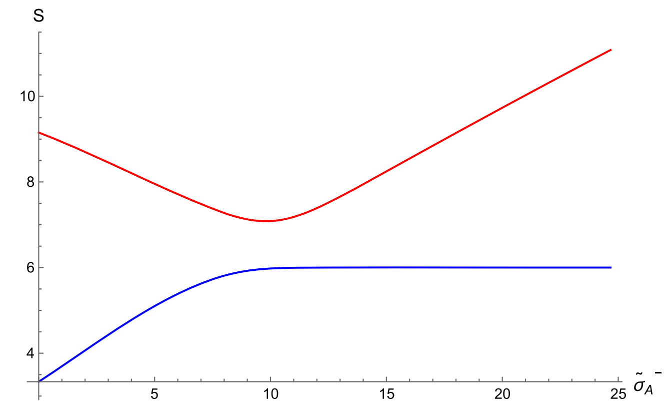

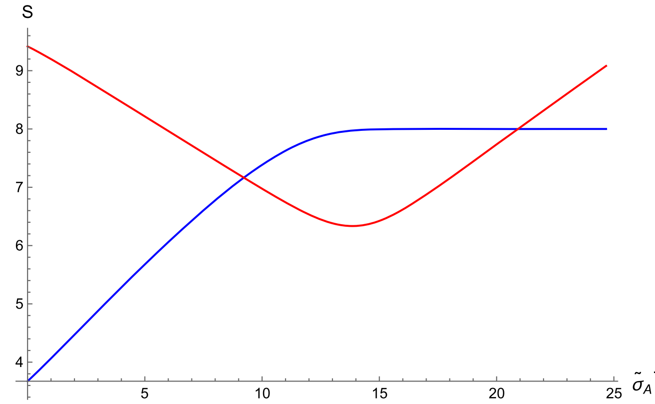

FIG. 8. Time evolution of the generalized entropy due to the Hawking (blue) and island (red) saddles, with $M = 7$ and $L_{AB} = 12$ (left), 16 (right). An entanglement dip appears for interval sizes above a critical value.

This condition yields a boundary "singularity" in the geometry, specified by the curve $\Omega(w^+, w^-) = \frac{1}{4}$. For the single-sided evaporating black hole, this singularity consists of a timelike and a spacelike portion (see Fig. 7). The former can naturally be viewed as the origin of radial coordinates in a higher-dimensional setting and where one simply imposes reflecting boundary conditions on the N matter fields $\{\psi_{k\pm}\}$ upon dimensional reduction. Therefore, we are dealing with a boundary conformal field theory (BCFT) for the matter fields. The spacelike portion of the curve $\Omega(w^+, w^-) = \frac{1}{4}$ is naturally interpreted as the black hole singularity behind the horizon. Consistent with this picture, for the eternal black hole the extended spacetime has no timelike boundary, and $\Omega(w^+, w^-) = \frac{1}{4}$ yields the spacelike singularities cloaked behind the past and future horizons as depicted in Fig. 8.

The action (3.5) has a residual gauge symmetry, which can be fixed by making the following choice

$$\chi = \Omega, \tag{3.7}$$

which turns out to describe the geometry in Kruskal coordinates. In this gauge, the dilaton and the generalized area can be expressed in terms of the conformal factor as

$$\phi = \rho_K - \frac{1}{2}\log\frac{N}{12}, \tag{3.8}$$

$$\Omega = e^{-2\rho_K} + \frac{1}{2}(\rho_K - \log 2). \tag{3.9}$$

The generalized area is determined by the equation of motion

$$\partial_+\partial_-\Omega = -1, \tag{3.10}$$

together with a constraint following from the semiclassical Einstein equations,

$$\partial_\pm^2\,\Omega = -\langle T_{\pm\pm}\rangle. \tag{3.11}$$

where on the right-hand side (rhs) we have the expectation value of the rescaled energy-momentum tensor

$$T_{\pm\pm} = \frac{6}{N}\sum_{k=1}^{N} i\psi_{k\pm}\partial_\pm\psi_{k\pm}, \tag{3.12}$$

normal ordered with respect to the Kruskal vacuum state, containing no positive-frequency modes with respect to the Kruskal time.

B. Evaporating black hole

Before analysing the entanglement entropy of a finite-size radiation subregion R at $\mathscr{I}^+$ in the case of an evaporating black hole, let us review the main features of the solution itself.

An evaporating black hole can be created by sending in a null pulse of energy M at $w^+ = 1$, and the corresponding geometry, following from Eqs. (3.10) and (3.11), is described by,[11]

$$\Omega(w^+, w^-) = -w^+w^- - \frac{1}{4}\log(-4w^+w^-) - M(w^+ - 1)\Theta(w^+ - 1). \tag{3.13}$$

The edge of spacetime, given by the curve $\Omega = \frac{1}{4}$ as explained above, is timelike behind the shockwave. On this portion we impose reflecting boundary conditions on the matter fields. It becomes spacelike after impact with the shockwave—this portion is interpreted as the black hole singularity, after which the boundary becomes timelike again at the end point when the black hole has evaporated completely.

[11]We follow the conventions adopted in literature on the RST model, e.g., [11] corresponding to a late time inverse Hawking temperature of $\beta = 2\pi$. In these units, the mass M of the black hole is dimensionless.

The evaporating black hole solution (3.13) has an apparent horizon, defined as the boundary of the trapped points, explicitly

$$\partial_+\Omega = 0 \Rightarrow w^+(w^- + M) = -\frac{1}{4}, \qquad w^+ > 1, \tag{3.14}$$

and the end of evaporation is given by the intersection of the apparent horizon with the black hole singularity,

$$w^-_{\mathrm{EP}} = \frac{M}{e^{-4M} - 1}, \qquad w^+_{\mathrm{EP}} = \frac{1}{4M}(e^{4M} - 1). \tag{3.15}$$

The event horizon will be defined by $w^- = w^-_{\mathrm{EP}}$.

The "in" vacuum for the fields is determined by the background at $\mathscr{I}^-$,

$$e^{2\rho_K}|_{w^-\to-\infty} = -\frac{1}{w^+w^-} + \frac{M}{(w^-)^2}\frac{(w^+-1)}{(w^+)^2} + O\left(\frac{1}{(w^-)^3}\right), \tag{3.16}$$

which corresponds to the linear dilaton "Minkowski" vacuum [10,11]. The "out" vacuum, on the other hand, is fixed by asymptotics at $\mathscr{I}^+$,

$$e^{2\rho_K}|_{w^+\to\infty} = -\frac{1}{w^+(w^- + M)} + O\left(\frac{1}{(w^+)^2}\right). \tag{3.17}$$

The natural outgoing Minkowski coordinates, using the same formalism as in [15], are

$$e^{\tilde{\sigma}^+} = w^+, \qquad -e^{-\tilde{\sigma}^-} = w^- + M, \tag{3.18}$$

related to the incoming coordinates,

$$w^\pm = \pm e^{\pm\sigma^\pm}. \tag{3.19}$$

Equivalently,

$$\tilde{\sigma}^+ = \sigma^+, \qquad \tilde{\sigma}^- = \sigma^- - \log(1 - Me^{\sigma^-}). \tag{3.20}$$

The end point of evaporation in these two sets of coordinates is

$$\begin{aligned} &\sigma^+_{\mathrm{EP}} = \tilde{\sigma}^+_{\mathrm{EP}} = 4M - \log 4M + \log(1 - e^{-4M}), \\ &\sigma^-_{\mathrm{EP}} = -\log M + \log(1 - e^{-4M}), \qquad \tilde{\sigma}^-_{\mathrm{EP}} = 4M + \sigma^-_{\mathrm{EP}}. \end{aligned} \tag{3.21}$$

1. Finite interval radiation entropy

The overall state is pure on any everywhere-spacelike or null slice stretching from spatial infinity to the timelike portion of the boundary singularity $\Omega = \frac{1}{4}$, at which we impose reflecting boundary conditions on the matter fields $\{\psi_k\}$.

The analogous problem, analysed above for the case of a black hole in JT gravity in thermal equilibrium with finite-size radiation intervals in the bath, can be rephrased in RST gravity's evaporating black hole scenario by considering a finite-size radiation interval at $\mathscr{I}^+$.

As a preliminary step, let us consider an interval $R \equiv [P_A, P_B]$ on a slice (prior to the future light cone of the evaporation end point) of the type described above. The quantum state on R is a density matrix ρ_R obtained by tracing over all the degrees of freedom of the slice outside R. With reflecting boundary conditions, the single-interval entanglement entropy in a BCFT can be viewed as the two-interval entanglement entropy of a chiral CFT on the plane. This was also extensively explained in [11]. Thus the entanglement entropy $S_{\mathrm{ent}}(R) = -\mathrm{Tr}(\rho_R \log \rho_R)$ is actually the entropy of *two disjoint intervals*, one corresponding to the direct null projection of R on $\mathscr{I}^-$ and the other obtained by considering the reflection of R across the timelike boundary, projected on $\mathscr{I}^-$.

On $\mathscr{I}^-$ the quantum fields are in their vacuum state, therefore for the entanglement entropy calculation, we can employ the free fermion results found in [20].[12] The quantum extremal prescription imposes that, in order to compute the generalized entropy of R, we need to take into account an island region as well, which we will denote as I, extending from the timelike boundary singularity to a point P_Q on the same Cauchy slice as the finite radiation interval. Therefore, our central object will be

$$S(R) = \min \mathrm{ext}_{P_Q}[S_{\mathrm{grav}}(P_Q) + S_{\mathrm{CFT}}(I \cup R)], \tag{3.22}$$

where

$$\begin{aligned} S_{\mathrm{grav}}(P_Q) = &\frac{N}{6}\left(e^{-2\rho_K(P_Q)} - \frac{\rho_K(P_Q)}{2}\right) \\ &+ \frac{N}{24}(\log 4 - 1) + \frac{N}{6}\log \epsilon_{\mathrm{UV}}, \end{aligned} \tag{3.23}$$

such that S_{grav} is the area term in RST gravity [11,15], and the CFT entanglement entropy of $I \cup R$ corresponds to the entanglement entropy of *three* disjoint intervals of finite size in a chiral (left-moving) CFT, namely

$$\begin{aligned} S_{\mathrm{CFT}}(I \cup R) = &\frac{N}{6}(\rho_{\mathrm{in}}(P_Q) + \rho_{\mathrm{in}}(P_A) + \rho_{\mathrm{in}}(P_B))) - \frac{N}{2}\log(\epsilon_{\mathrm{UV}}) \\ &+ \frac{N}{6}\left[\sum_{i,j}\log|u_i - v_j| - \sum_{i<j}\log|u_i - u_j| - \sum_{i<j}\log|v_i - v_j|\right] \end{aligned} \tag{3.24}$$

[12] In the presence of a shockwave, as in our case, it is sufficient to consider a coherent state of matter fields, and the same formulas apply.

with

$$[u_1, v_1] = [\sigma^+_{\bar{B}}, \sigma^+_{\bar{A}}], \qquad [u_2, v_2] = [\sigma^+_{\bar{Q}}, \sigma^+_{Q}], \qquad [u_3, v_3] = [\sigma^+_{A}, \sigma^+_{B}]. \tag{3.25}$$

Here we note that the incoming Minkowski coordinate of the null ray which reaches a point P, after reflecting off the boundary at $\Omega = \frac{1}{4}$, is given by

$$\sigma^+_{\bar{P}} = \sigma^-_{P} - \log 4. \tag{3.26}$$

Since we want the observer to collect the outgoing radiation at $\mathscr{I}^+$, we can move the Cauchy slice toward $\mathscr{I}^+$ by taking $\sigma^+_{A,B} \to +\infty$. The entanglement entropy of the outgoing radiation then only depends on the coordinates $\sigma^-_{A,B}$, or equivalently the reflected coordinates $\sigma^+_{\bar{A},\bar{B}}$ on $\mathscr{I}^-$, of the end points P_A and P_B. This yields the following expression for the CFT entanglement entropy of $I \cup R$,

$$S_{\mathrm{CFT}}(I \cup R) = \frac{N}{6} \log\left[\frac{(\sigma^+_{Q} - \sigma^+_{\bar{B}})(\sigma^+_{\bar{A}} - \sigma^+_{\bar{B}})(\sigma^+_{\bar{Q}} - \sigma^+_{\bar{A}})(\sigma^+_{Q} - \sigma^+_{\bar{Q}})}{\epsilon^2_{\mathrm{UV}} e^{-\rho_{\mathrm{in}}(P_A) - \rho_{\mathrm{in}}(P_B) - \rho_{\mathrm{in}}(P_Q)}(\sigma^+_{\bar{Q}} - \sigma^+_{\bar{B}})(\sigma^+_{Q} - \sigma^+_{\bar{A}})}\right], \tag{3.27}$$

where one factor of ϵ_{UV} factor is accounted for by taking $\sigma^+_A - \sigma^+_B \simeq \epsilon_{\mathrm{UV}}$.

The area term (3.23), evaluated at the QES P_Q, can be equivalently expressed as

$$S_{\mathrm{grav}}(P_Q) = \frac{N}{6}\left[\Omega(P_Q) - \rho_K(P_Q) + \log 2 - \frac{1}{4} + \log \epsilon_{\mathrm{UV}}\right],$$

by using Eq. (3.9).

Putting all together, the generalized entropy of $I \cup R$ takes the form

$$\begin{aligned} S_{\mathrm{gen}}(I \cup R) &= S_{\mathrm{grav}}(P_Q) + S_{\mathrm{CFT}}(I \cup R) \\ &= \frac{N}{6}\left[\Omega(P_Q) - \frac{1}{4} + \frac{1}{2}(\sigma^+_{Q} - \sigma^+_{\bar{Q}}) + \log(\sigma^+_{Q} - \sigma^+_{\bar{Q}}) + \log(\sigma^+_{Q} - \sigma^+_{\bar{B}})\right. \\ &\quad \left. + \log(\sigma^+_{\bar{Q}} - \sigma^+_{\bar{A}}) - \log(\sigma^+_{\bar{Q}} - \sigma^+_{\bar{B}}) - \log(\sigma^+_{Q} - \sigma^+_{\bar{A}})\right] + \frac{N}{6}\log\left[\frac{\sigma^+_{\bar{A}} - \sigma^+_{\bar{B}}}{\epsilon_{\mathrm{UV}}\sqrt{(1 - 4Me^{\sigma^+_{\bar{A}}})(1 - 4Me^{\sigma^+_{\bar{B}}})}}\right], \end{aligned} \tag{3.28}$$

where we used

$$\rho_{\mathrm{in}} = \rho_K + \frac{1}{2}(\sigma^+ - \sigma^-), \tag{3.29}$$

$$\rho_{\mathrm{in}}(P_i) = \log\left(\frac{1}{\sqrt{1 - 4Me^{\sigma^+_{\bar{i}}}}}\right), \qquad i = A, B. \tag{3.30}$$

The last line of Eq. (3.28) is the standard CFT result, the coarse-grained entanglement entropy, of the radiation interval R. The extremization of the generalized entropy with respect to QES coordinates $\sigma^+_{\bar{Q}}$ and σ^+_{Q} yields, respectively,

$$e^{(\sigma^+_{Q} - \sigma^+_{\bar{Q}})} + 1 + \frac{4}{\sigma^+_{Q} - \sigma^+_{\bar{Q}}} - \frac{4}{\sigma^+_{\bar{Q}} - \sigma^+_{\bar{A}}} + \frac{4}{\sigma^+_{\bar{Q}} - \sigma^+_{\bar{B}}} = 0, \tag{3.31}$$

$$e^{(\sigma^+_{Q} - \sigma^+_{\bar{Q}})} + 1 - 4Me^{\sigma^+_{Q}} + \frac{4}{\sigma^+_{Q} - \sigma^+_{\bar{Q}}} - \frac{4}{\sigma^+_{Q} - \sigma^+_{\bar{A}}} + \frac{4}{\sigma^+_{Q} - \sigma^+_{\bar{B}}} = 0. \tag{3.32}$$

Usually one is interested in the entropy of *all* radiation emitted by the black hole up to some fixed time in which case the radiation interval is effectively semi-infinite stretching from spacelike infinity to some point P on $\mathcal{I}^+$, and the Page curve is obtained as a function of the outgoing Minkowski coordinate of the end point $\tilde{\sigma}^-_P$ [15]. In our case, it is natural to pick the outgoing coordinate of the furthest end point $\tilde{\sigma}^-_A$ as the temporal dial, while the size of the interval is determined by the difference

$$L_{AB} \equiv \tilde{\sigma}_A^- - \tilde{\sigma}_B^-. \tag{3.33}$$

We will keep L_{AB} fixed while $\tilde{\sigma}_{A,B}^-$ both grow linearly with outgoing Minkowski time.

For large enough interval size $L_{AB} \gg 1$, the CFT or coarse-grained entropy for R first grows linearly and then saturates at late times,

$$S_{\mathrm{CFT}}(R) \simeq \begin{cases} \frac{N}{12}(\tilde{\sigma}_A^- + \log M + 2\log L_{AB}) & \tilde{\sigma}_A^- \ll L_{AB} - \log M, \\ \frac{N}{12} L_{AB} & \tilde{\sigma}_A^- \gtrsim L_{AB} - \log M. \end{cases} \tag{3.34}$$

This result from the no-island or Hawking saddle must be thought of as a balancing act between modes entering and modes leaving a finite sliding window: the end point A continually captures fresh Hawking modes, while the end point B lets older modes escape. At early times, as more modes enter the interval than escape, the Hawking entropy increases until the plateau time $\tilde{\sigma}_A^- \simeq L_{AB} - \log M$, at which point the entry and exit rates equalize, and the entropy of the interval saturates at the thermal value.[13]

Numerical solution of the QES equations (3.31) and (3.32) in the regime $M \gg 1$ shows that the QES rapidly settles close to the event horizon, located at $\sigma_{\mathrm{EP}}^- \simeq -\log M$. Taking the difference of Eqs. (3.31) and (3.32), we obtain,

$$e^{\sigma_Q^+} = \frac{1}{M}\left(\frac{1}{\sigma_Q^- - \tilde{\sigma}_A^- + \log(1 + Me^{\tilde{\sigma}_A^-})} - \frac{1}{\sigma_Q^- - \tilde{\sigma}_A^- + \log(e^{L_{AB}} + Me^{\tilde{\sigma}_A^-})}\right). \tag{3.35}$$

where we suppress the analogue σ_Q^+ terms on the rhs, since they are subleading *a posteriori*. Eqs. (3.35) and (3.31), at leading order then imply,

$$4e^{\sigma_Q^+}(e^{-\sigma_Q^-} - M) = 0, \tag{3.36}$$

which yields $\sigma_Q^- = -\log M$, agreeing with the numerical solutions. This solution for σ_Q^- along with (3.35) determines σ_Q^+

$$\sigma_Q^+ = \tilde{\sigma}_A^- - L_{AB} + \log(e^{L_{AB}} - 1) + \mathcal{O}\left(\frac{e^{-\tilde{\sigma}_A^-}}{M}\right). \tag{3.37}$$

In Fig. 8 we display the time evolution of the generalized entropy evaluated on the no-island (blue) and island (red) saddles, for two different values of L_{AB}, up to the end point of evaporation given by $\tilde{\sigma}_{A,\mathrm{fin}}^- = 4M - \log M + L_{AB} - \log(e^{L_{AB}} - 1)$, at which the QES hits the end point of evaporation (3.21). As we keep increasing the interval size, it turns out that the island saddle becomes more relevant, and for a larger time range. In the strict $L_{AB} \to +\infty$ limit, we recover the Page curve of a semi-infinite interval with $S_{\mathrm{gen}}(\tilde{\sigma}_{A,\mathrm{fin}}^-) = S_{\mathrm{gen}}(\tilde{\sigma}_{A,\mathrm{in}}^-)$ obtained in [15,24].

To find the critical interval length below which the island saddle is always subdominant and no entanglement dip appears, we first note that the difference between the generalized entropy evaluated on the island and the Hawking saddles takes the following form:

$$\frac{6\Delta S}{N} \simeq M - \frac{3}{4}(\log M + \tilde{\sigma}_A^-) + \log\left[\frac{L_{AB} + \log 4 + \log(1 + Me^{-L_{AB} + \tilde{\sigma}_A^-})}{L_{AB} - \tilde{\sigma}_A^- - \log M + \log(1 + Me^{-L_{AB} + \tilde{\sigma}_A^-})}\right], \tag{3.38}$$

where we have used $L_{AB} \gg 1$. We will see that this is justified *a posteriori* as the critical value for L_{AB} is $\mathcal{O}(M)$. The minimum of ΔS is located at $\tilde{\sigma}_A^- \simeq L_{AB} - \log M$, with value

$$\frac{6\Delta S_{\min}}{N} = M - \frac{3}{4}L_{AB} + \log L_{AB} + \mathcal{O}(M^0). \tag{3.39}$$

The island and Hawking saddles give comparable entropy contributions for $L_{AB} \gtrsim M$ as expected. In particular, the critical length above which a dip appears, satisfying $\Delta S_{\min} = 0$, is

$$L_{AB}^{\mathrm{crit}} \simeq -\frac{4}{3}W_{-1}\left(-\frac{3}{4}e^{-M}\right) = \frac{4}{3}(M + \log M) + \mathcal{O}(M^0), \tag{3.40}$$

here $W_k(x)$ is the product logarithm function.[14]

However, note that, in the RST model, the scrambling time and mass of the black hole are related via [11]

$$t_{\mathrm{scr}} = \frac{\beta}{2\pi}\log\frac{S_{\mathrm{BH}}}{N} = \log\frac{M}{6}, \tag{3.41}$$

[13]From the one-point function for the stress tensor, it can be readily deduced that the evaporating RST black hole has an effective time dependent temperature that quickly settles to a constant value $\beta^{-1} \approx 1/2\pi$. The thermal entropy of a large interval of size L is then simply $\pi NL/6\beta$, matching (3.34).

[14]It is implicitly defined through $W_k(x)e^{W_k(x)} = x$ and k indicates choice of branch of the function.

recalling that $\beta = 2\pi$ and $S_{\rm BH} = \frac{NM}{6}$. Therefore in terms of scrambling time we can express the critical length as follows

$$L_{AB}^{\rm crit} = 8e^{t_{\rm scr}} + \frac{4}{3}t_{\rm scr} + \mathcal{O}(1). \tag{3.42}$$

In addition, we can also compute the Page time when the entanglement dip begins ($\Delta S = 0$) for any fixed L_{AB}, assuming $L_{AB} > L_{AB}^{\rm crit}$,

$$\tilde{\sigma}^-_{A,\rm Page} \simeq L_{AB} - \log M + \frac{4}{3}W_{-1}\left(-\frac{3}{4}e^{M-\frac{3}{4}L_{AB}}L_{AB}\right). \tag{3.43}$$

The reality of the last term imposes the minimum or critical length requirement on L_{AB}. In the $L_{AB} \to +\infty$, we recover the Page time for the semi-infinite radiation interval [15],

$$\tilde{\sigma}^-_{A,\rm Page}(L_{AB} \to +\infty) \simeq \frac{4}{3}M - \log M. \tag{3.44}$$

2. *Interpretation of dip and rise*

When the island saddle becomes dominant, the entanglement book-keeping changes. The QES rapidly approaches the event horizon, and its outgoing coordinate σ_Q^+, tracks the radiation window as per (3.37). In this way, the island captures the purifying partners of a subset of the Hawking quanta contained in R, and the fine-grained entropy decreases.

However, for a finite interval, this purification is only temporary. As the coordinates $\tilde{\sigma}^-_{A,B}$ of the two end points describe a sliding interval of field size, the radiation window keeps moving. Some Hawking modes that were purified by the island eventually leave the interval through the end point B. Once they are no longer in R, the corresponding purification is lost from the entropy of $I \cup R$, and the island branch can rise again. This explains the second rise: it is a finite-window effect caused by already-purified Hawking modes escaping the radiation interval.

Following the dip and the rise, generically the single interval entanglement entropy will saturate at its thermal value. For L_{AB} large enough, this loss through B is postponed beyond the evaporation regime, and the second rise disappears, getting a Page-curve behavior, analogous to the one of a semi-infinite radiation region.

On the other hand, if we consider increasingly small radiation intervals, there is a critical size dictated by Eq. (3.40) below which the interval never contains enough Hawking quanta for the partial purification to compensate the gravitational cost of including the island, i.e. the island saddle is never dominant and the radiation is maximally scrambled.

C. Eternal RST black hole and entanglement revival

The solution for the eternal black hole in the RST model (see Fig. 9) is given by

$$\Omega = -w^+w^- + M, \tag{3.45}$$

satisfying Eqs. (3.10) and (3.11) with $\langle T_{\pm\pm}\rangle = 0$. The Kruskal coordinates are defined as in the AdS$_2$ case (2.2), with the only difference being that the inverse temperature is fixed to $\beta = 2\pi$.

Similarly to the JT gravity-plus-bath system, we now consider two symmetric intervals on $\mathscr{I}^+$, with $a, b \gg 1$, as forming the radiation system. The calculation of the generalized entanglement entropy, including the island contribution, follows the exact same steps as in the JT case. The main differences arise in the area (Bekenstein-Hawking) contribution to the generalized entropy and the conformal factors at the end points of the intervals, respectively given as,

$$S_{\rm grav} = \frac{N}{6}\left(e^{-2\rho_K} - \frac{\rho_K}{2}\right) + \frac{N}{24}(\log 4 - 1) + \frac{N}{6}\log \epsilon_{\rm UV}, \tag{3.46}$$

$$S_{\rm conf} = \frac{N}{6}\rho_K - \frac{N}{6}\log \epsilon_{\rm UV}. \tag{3.47}$$

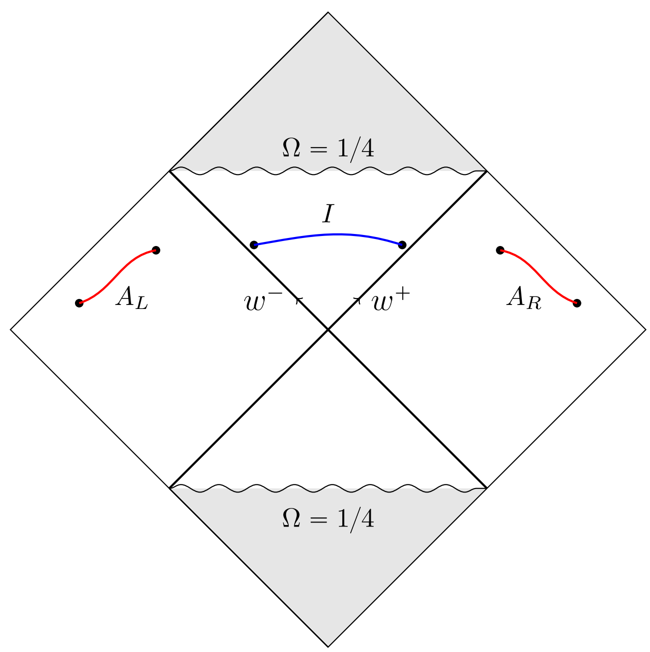

FIG. 9. Eternal black hole described by the solution (3.45) of the RST model. Now, the $\Omega = 1/4$ curve is spacelike everywhere and represents the singularity behind the horizon, depicted by wavy lines.

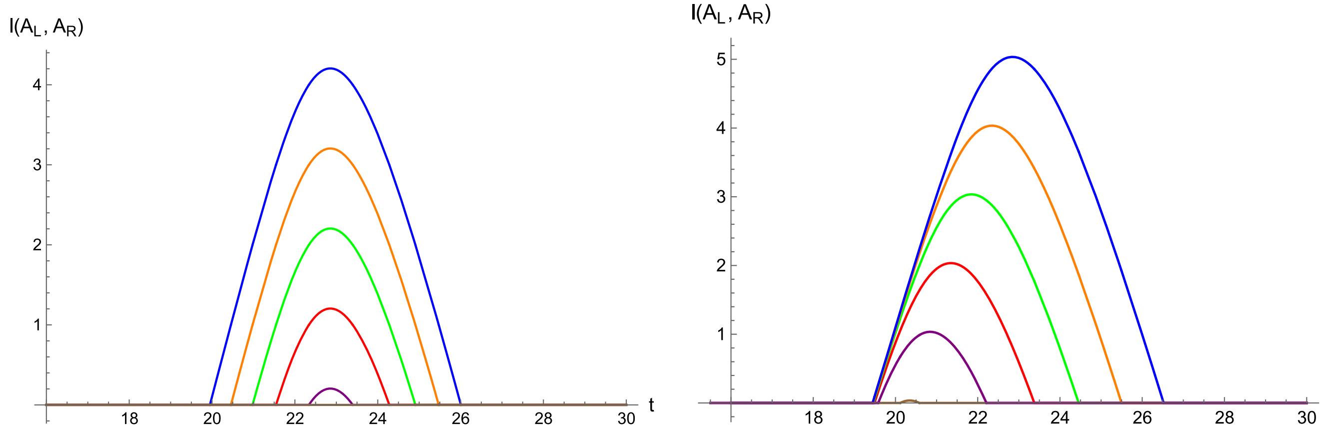

FIG. 10. Depiction of the mutual information $I(A_L, A_R)$ after the entropic early-time growth regime. Left: the size of the intervals is fixed, with $a = 16$ and $b = 30$, and the black hole mass increases from the top curve in blue ($M = 3.5$) to the bottom curve ($M = 6$) in steps of 0.5. Right: the black hole mass and one end point of each of the two symmetric intervals is kept fixed, $M = 3$ and $a = 16$, while the size of the intervals is decreased, starting with $b = 29$ up to $b = 24$ in steps of 1.

Given two symmetrically located QESs, the expression for the generalized entropy in the presence of an island is then,

$$S_{\rm gen}(I\cup R) = \frac{N}{3}\left[\Omega(w^{\pm}_{2_Q}) - \frac{1}{4} - \log\frac{\epsilon^2_{\rm UV}}{2} + \rho_K(w^{\pm}_{1_R}) + \rho_K(w^{\pm}_{2_R})\right] + S^{\rm flat}_{\rm CFT}(I\cup R), \tag{3.48}$$

where $S^{\rm flat}_{\rm CFT}(I\cup R)$ is the flat space, vacuum entanglement entropy of $I\cup R$ [20], identical to corresponding terms in the JT-gravity case (2.15).

The extremization conditions with respect to the QES coordinates $w^{\pm}_{2_Q}$, in the high temperature/large interval limit, are the same as Eq. (2.19), with the replacement $(s+1)/s \to 1$. The coordinate $w^{+}_{2_Q}$ of the right QES is

$$w^{+}_{2_Q} \approx \begin{cases} e^{t-a} & a < t \lesssim \frac{a+b}{2}, \\ e^{(b-a)/2} & \frac{a+b}{2} \lesssim t < b. \end{cases} \tag{3.49}$$

Restoring the temperature dependence, this is essentially the same as.(6) The difference between the island and no-island generalized entropies is

$$\frac{6\Delta S}{N} \approx 2M - 2w^{+}_{2_Q}w^{-}_{2_Q} + 2\log 2 - \frac{1}{2} + 2\log\left(e^{t-b} + \frac{1}{w^{+}_{2_Q}}\right). \tag{3.50}$$

The location of the dip is found by minimizing ΔS with respect to time,

$$t_{\rm min} = \frac{a+b}{2} + \mathcal{O}(M^0), \tag{3.51}$$

and the effect disappears for interval length below a critical value,

$$L_{\rm crit} = 2M + \mathcal{O}(M^0) = 12e^{t_{\rm scr}} + \mathcal{O}(1), \tag{3.52}$$

where in the second equality we used the relation between mass and scrambling time in the RST model stated in Eq. (3.41). Interestingly, in contrast to (2.28) and (2.31) for the AdS_2 case in JT-gravity, the location of the dip and critical length both do not display $\mathcal{O}(t_{\rm scr})$ corrections.

In Fig. 10, we plot the results for the mutual information $I(A_L, A_R)$ of the left and right radiation intervals by keeping L_{AB} fixed and varying the black hole mass M, and vice versa. As expected from our analytical result (3.52), entanglement memory progressively disappears upon either increasing the scrambling time or shrinking the interval length. The absence of $\mathcal{O}(t_{\rm scr})$ corrections to the $t_{\rm min}$ makes the mutual information peak appear symmetric about the midpoint unlike the situation in JT gravity. Moreover, the end points are found to be

$$t_{\rm in} = a + M + \mathcal{O}(1), \qquad t_{\rm fin} = b - M + \mathcal{O}(1), \tag{3.53}$$

again without $\mathcal{O}(t_{\rm scr})$ corrections.

We focussed above on the case $b < 3a$, while for the case $b > 3a$, analogous results to the ones found in Sec. II C 1 follow: in particular the critical mass for the disappearance of regime (II) is

$$M^{\rm (II)}_{\rm crit} = \frac{b-3a}{2}. \tag{3.54}$$

IV. CONCLUSIONS AND OPEN QUESTIONS

We studied the entanglement evolution of finite, equal-size intervals in 2D CFT prepared in the thermofield double state, viewing CFT degrees of freedom as radiation modes of evaporating black holes. The black holes under consideration are solutions of two well-known 2D dilaton gravity theories: JT gravity and RST gravity. For the JT case, we considered an eternal black hole coupled to flat space baths CFT_L and CFT_R in the high-temperature limit (in the TFD state). For the RST model, we analyzed both an evaporating black hole with a finite radiation interval on $\mathscr{I}^+$ and the corresponding eternal black hole setup. In each case, we computed the fine-grained entropy and the mutual information, investigating how island-induced purification effects are modified by the interplay between the interval size and the scrambling time.

The general lesson from both these setups is that entanglement revival sets in for length scales larger than the exponential of the black hole scrambling time with $\mathcal{O}(t_{\mathrm{scr}})$ corrections (1.2). This is, of course, not unexpected as the Page time itself scales with the entropy of the black hole. The critical length scale, however, also provides a measure of the length scale above which long-range correlations in the radiation become detectable.

There are a few different questions of interest following on from our work. In the limit of zero scrambling time and high temperatures, the entanglement structure of two disjoint finite intervals A_L and A_R in JT gravity coupled to free Minkowski CFT baths, precisely matches the entanglement evolution of free BCFTs in the TFD state [18]. In this situation the appearance of the dip can be explained through modes reflecting off the boundary in either copy, entering A_L and A_R along with their respective purifiers in the TFD copy. It would be interesting to find the correct extension or modification of this geometric picture once the scrambling effects become relevant: in particular the arguments in [25] suggest that the boundary behaves as if it has an effective thickness $\epsilon \sim \frac{1}{k}$. We would then expect rays meeting the boundary to undergo a delay and/or clipping effect, which could potentially explain our results for the end points of the dip (or mutual information spike) being shifted inward by an amount $\frac{1}{2k}$, which is actually exponential in scrambling time. This is the case in both JT and RST models seen in Eqs. (2.33) and (3.53). Exploring this connection could also provide a route to incorporating the effects of finite scrambling time of the boundary theory on the modular Hamiltonian of the free BCFT [26].

Our focus in this paper was on the free fermion CFT with scrambling induced purely by the black hole, or in the holographic dual description by a boundary SYK-like chaotic system (for a closely related setting see [27,28]). For maximally scrambling holographic large-c CFTs we know that entanglement revivals are absent with or without a black hole [4,6,29]. In principle it would be more interesting to look at situations where the radiation system was neither free nor maximally scrambling, so the interplay between the scrambling times of the radiation system and black hole could be investigated in more detail [30–32]. This type of situation could potentially be explored by considering the SYK system coupled to interacting spin chains, for instance [33].

ACKNOWLEDGMENTS

The authors would like to thank Tim Hollowood for discussions. S. P. K. would like to acknowledge support from STFC Consolidated Grant Award No. ST/X000648/1. N. B. is supported by the STFC DTP Grant Reference No. ST/Y509644/1. L. B. N. B. is supported by EPSRC Grant No. EP/W524694/1 and STFC Grant No. ST/Y509644/1.

DATA AVAILABILITY

There are no publicly available research data or software supporting this manuscript. Requests for further information or data should be sent to the authors.

[1] P. Hayden and J. Preskill, Black holes as mirrors: Quantum information in random subsystems, J. High Energy Phys. 09 (2007) 120.

[2] Y. Sekino and L. Susskind, Fast scramblers, J. High Energy Phys. 10 (2008) 065.

[3] S. H. Shenker and D. Stanford, Black holes and the butterfly effect, J. High Energy Phys. 03 (2014) 067.

[4] C. T. Asplund, A. Bernamonti, F. Galli, and T. Hartman, Entanglement scrambling in 2d conformal field theory, J. High Energy Phys. 09 (2015) 110.

[5] P. Calabrese and J. Cardy, Entanglement entropy and conformal field theory, J. Phys. A **42**, 504005 (2009).

[6] C. T. Asplund and A. Bernamonti, Mutual information after a local quench in conformal field theory, Phys. Rev. D **89**, 066015 (2014).

[7] S. Leichenauer and M. Moosa, Entanglement Tsunami in $(1+1)$-dimensions, Phys. Rev. D **92**, 126004 (2015).

[8] R. Jackiw, Lower dimensional gravity, Nucl. Phys. **B252**, 343 (1985).

[9] C. Teitelboim, Gravitation and Hamiltonian structure in two space-time dimensions, Phys. Lett. **126B**, 41 (1983).

[10] J. G. Russo, L. Susskind, and L. Thorlacius, The endpoint of Hawking radiation, Phys. Rev. D **46**, 3444 (1992).

[11] T. M. Fiola, J. Preskill, A. Strominger, and S. P. Trivedi, Black hole thermodynamics and information loss in two-dimensions, Phys. Rev. D **50**, 3987 (1994).

[12] A. Almheiri, R. Mahajan, and J. Maldacena, Islands outside the horizon, arXiv:1910.11077.

[13] A. Almheiri, T. Hartman, J. Maldacena, E. Shaghoulian, and A. Tajdini, Replica wormholes and the entropy of Hawking radiation, J. High Energy Phys. 05 (2020) 013.

[14] G. Penington, S. H. Shenker, D. Stanford, and Z. Yang, Replica wormholes and the black hole interior, J. High Energy Phys. 03 (2022) 205.

[15] T. Hartman, E. Shaghoulian, and A. Strominger, Islands in asymptotically Flat 2D gravity, J. High Energy Phys. 07 (2020) 022.

[16] S. Leichenauer, Disrupting entanglement of black holes, Phys. Rev. D **90**, 046009 (2014).

[17] E. Perlmutter, Bounding the space of holographic CFTs with chaos, J. High Energy Phys. 10 (2016) 069.

[18] T. J. Hollowood, S. P. Kumar, A. Legramandi, and N. Talwar, Ephemeral islands, plunging quantum extremal surfaces and BCFT channels, J. High Energy Phys. 01 (2022) 078.

[19] T. G. Mertens and G. J. Turiaci, Solvable models of quantum black holes: A review on Jackiw–Teitelboim gravity, Living Rev. Relativity **26**, 4 (2023).

[20] H. Casini and M. Huerta, Entanglement entropy in free quantum field theory, J. Phys. A **42**, 504007 (2009).

[21] C. G. Callan, Jr., S. B. Giddings, J. A. Harvey, and A. Strominger, Evanescent black holes, Phys. Rev. D **45**, R1005 (1992).

[22] D. A. Lowe, Semiclassical approach to black hole evaporation, Phys. Rev. D **47**, 2446 (1993).

[23] T. Piran and A. Strominger, Numerical analysis of black hole evaporation, Phys. Rev. D **48**, 4729 (1993).

[24] F. F. Gautason, L. Schneiderbauer, W. Sybesma, and L. Thorlacius, Page curve for an evaporating black hole, J. High Energy Phys. 05 (2020) 091.

[25] N. Callebaut and H. Verlinde, Entanglement dynamics in 2D CFT with boundary: Entropic origin of JT gravity and Schwarzian QM, J. High Energy Phys. 05 (2019) 045.

[26] I. A. Reyes, Moving mirrors, Page curves, and bulk entropies in AdS_2, Phys. Rev. Lett. **127**, 051602 (2021).

[27] F. Fritzsch and T. Prosen, Boundary chaos, Phys. Rev. E **106**, 014210 (2022).

[28] F. Fritzsch, R. Ghosh, and T. Prosen, Boundary chaos: Exact entanglement dynamics, SciPost Phys. **15**, 092 (2023).

[29] V. Balasubramanian, B. Craps, M. Khramtsov, and E. Shaghoulian, Submerging islands through thermalization, J. High Energy Phys. 10 (2021) 048.

[30] H. Liu and S. Vardhan, A dynamical mechanism for the Page curve from quantum chaos, J. High Energy Phys. 03 (2021) 088.

[31] Y. Gu, A. Lucas, and X. L. Qi, Spread of entanglement in a Sachdev-Ye-Kitaev chain, J. High Energy Phys. 09 (2017) 120.

[32] Y. Chen, H. Zhai, and P. Zhang, Tunable quantum chaos in the Sachdev-Ye-Kitaev model coupled to a thermal bath, J. High Energy Phys. 07 (2017) 150.

[33] Y. Chen, X. L. Qi, and P. Zhang, Replica wormhole and information retrieval in the SYK model coupled to Majorana chains, J. High Energy Phys. 06 (2020) 121.